http://dx.doi.org/10.21577/0100-4042.20170465 *Quim. Nova,* Vol. 43, No. 2, 188-193, 2020

Artigo

JUDD-OFELT ANALYSIS OF Tb^{3+} AND UPCONVERSION STUDY IN Yb^{3+}–Tb^{3+} CO-DOPED CALIBO GLASSES

Idelma A. A. Terra[a], Luis J. Borrero-González[b,*], Juliana M. P. Almeida[a], Antonio C. Hernandes[a] and Luiz A. O. Nunes[a,#]
[a]Instituto de Física de São Carlos, Universidade de São Paulo, 13560-970 São Carlos – SP, Brasil
[b]Escuela de Ciencias Físicas y Matemática, Facultad de Ciencias Exactas y Naturales, Pontificia Universidad Católica del Ecuador, Apartado postal 17012184, Quito, Ecuador

Recebido em 19/08/2019; aceito em 22/10/2019; publicado na web em 22/01/2020

We report on the study of the spectroscopic properties in Ytterbium–Terbium (Yb^{3+}-Tb^{3+}) co-doped calcium lithium borate (CaLiBO) glasses, with the study's focus being on the upconversion process. Intensity parameters Ω_λ for CaLiBO:Tb^{3+} are determined by the Judd–Ofelt method to be $\Omega_2 = 15.5 \times 10^{-20}$ cm^2, $\Omega_4 = 1.90 \times 10^{-20}$ cm^2 and $\Omega_6 = 3.69 \times 10^{-20}$ cm^2. We have also obtained electric-dipole (and magnetic-dipole) radiative transition probabilities, branching ratios, and lifetime for the Tb^{3+}:$^5D_4$ and $^5D_3$ levels. In addition, an evaluation of the upconversion processes by luminescence and time-resolved spectroscopy were carried out. The upconversion rise and decay times, energy transfer probability from Yb^{3+} to Tb^{3+} ions, and the efficiency of the processes that depopulate the Tb^{3+}:$^5D_4$ level after resonantly pumping the Yb^{3+}:$^2F_{5/2}$ level were estimated. Our results showed that a cooperative energy transfer (CET) from two Yb^{3+} ions to one Tb^{3+} ion is the origin of the Tb^{3+} upconversion luminescence in the visible region. While, CET followed of the cross relaxation or/and excited state absorption is responsible for the upconversion luminescence in the ultraviolet region.

Keywords: Judd-Ofelt analysis; upconversion; CaLiBO glasses; rare earth ions; luminescence.

INTRODUCTION

The study of optical properties such as absorption, luminescence, and in particular, the energy transfer processes in lanthanide-ion-doped materials is fundamental. This is due to their potential applications in, for example, bio-sensing and bio-imaging,[1] photovoltaics,[2] and solid state lasers.[3] The downconversion (DC) and upconversion (UC) processes have been widely studied, starting with the first theoretical proposals by Dexter[4] and Auzel,[5] respectively. The UC luminescence in Yb^{3+}-Tb^{3+} co-doped glasses was first observed by Livanova *et al.* in 1969.[6] This ion-pair interaction between Yb^{3+} (donor) and Tb^{3+} (acceptor) is known to lead to a simultaneous energy conversion of two near-infrared (NIR) photons into one visible photon after pumping the Yb^{3+}:$^2F_{5/2}$ level. The photon energy conversion has been explained in terms of a cooperative energy transfer (CET) process attributed to $2Yb^{3+}$:$^2F_{5/2} \rightarrow {}^2F_{7/2}$; Tb^{3+}:$^7F_6 \rightarrow {}^5D_4$.[7–9] This is also a non-resonant phonon-assisted process, confirmed by the study of the dependence of the Tb^{3+} UC visible luminescence with temperatures in the range of 10-300 K.[10,11] The Yb^{3+} ions are used as donors both due to the high absorption cross-section, and because the Yb^{3+}:$^2F_{5/2}$ level acts as a population reservoir when pumping with 980 nm.[12] These characteristics are important in regard to the UC process.

Among the various existing options, calcium lithium borate (CaLiBO) glasses are promising hosts for examining the effects of chemical environments on the optical properties of the lanthanides ions, due to their high transparency, low melting point, and high thermal stability.[13] Another important characteristic of these glasses is their acceptance for a large concentration of lanthanides ions. Some authors have studied the energy transfer process in Dy^{3+}-Ho^{3+}, Tb^{3+}-Er^{3+}, Sm^{3+}-Eu^{3+}, Tb^{3+}-Ho^{3+}, Dy^{3+}-Nd^{3+}, Eu^{3+}-Pr^{3+}, and Eu^{3+}-Ho^{3+} co-doped CaLiBO glasses.[13–19] We have studied the DC process in Tb^{3+}-Yb^{3+} co-doped CaLiBO glasses.[20] However, to the best of our knowledge, the UC process in Yb^{3+}-Tb^{3+} co-doped CaLiBO glasses has not yet been investigated. Moreover, a scarce spectroscopic analysis in Tb^{3+} doped CaLiBO glass is reported[21–23] and a few works reports on the determination of energy transfer probabilities from Yb^{3+} to Tb^{3+}. The novelty of this work is the unequivocal determination of these values through the study of the UC luminescence kinetics. Therefore, CaLiBO glass was selected as the host material for the analysis of the UC processes in the Yb^{3+}-Tb^{3+} system, prioritizing the studies of the influence of the variation of dopant concentrations on the system's optical properties.

A set of Yb^{3+}-Tb^{3+} co-doped CaLiBO glasses with Yb^{3+} concentration from (0 to 7)% mol and with Tb^{3+} concentration fixed at 0.5% mol were studied. The spectroscopic characteristics of the glasses were investigated by absorption, luminescence and time-resolved spectroscopy measurements. The upconversion rise and decay times, energy transfer probability from Yb^{3+} to Tb^{3+} ions, and the efficiency of the processes that depopulate the Tb^{3+}:$^5D_4$ level after pumping the Yb^{3+}:$^7F_{5/2}$ level using a 5-ns pulsed laser as the excitation source were estimated.

EXPERIMENTAL

Synthesis of glasses

A CaLiBO glass matrix ($30CaO + 10Li_2O + 60B_2O_3$) (% mol) was prepared by the conventional melt-quenching method using high-purity $CaCO_3$, Li_2CO_3, and B_2O_3, this glass was then doped with Tb_4O_7 and Yb_2O_3, at approximately 1200 ºC for 1 h. The set of CaLiBO glasses doped with Tb_4O_7 and Yb_2O_3 were prepared with the following compositions: $(99.5\text{-}x)\%$ CaLiBO + 0.5% $Tb_4O_7 + x\,Yb_2O_3$, with x = 0, 0.1, 0.5, 1, 2.5, 5, and 7 (% mol). The glasses were cut and polished into a plate shape with the following dimensions: 3 mm × 10 mm × 10 mm.

Optical characterization

Ground state absorption spectra for both sets of samples were obtained using a Perkin Elmer Lambda 900 spectrophotometer in the 250-2500 nm spectral range. The visible Stokes luminescence spectra

*e-mail: ljborrero@puce.edu.ec
#e-mail alternativo: luizant@ifsc.usp.br

were obtained using a He-Cd laser (Kimmon/IK5652R-G) at 325 nm as the excitation source. The luminescent signal was dispersed by a monochromator (0.3 m, Thermo Jarrel Ash/82497), detected by a photomultiplier tube (PMT) (Hamamatsu/R928), and amplified by a lock-in amplifier. The UC luminescence spectra were obtained using an InGaAs index-guided strained-layer diode laser (Coherent, 980 nm excitation wavelength) as the excitation source, and the same laser was employed for the excitation power dependent measurements. Tb^{3+}:$^5D_4$ $^7F_5$ UC luminescence kinetic response measurements were performed using an optical parametrical oscillator (OPO) (Surelite SLOP/Continumm) pumped by the third harmonic (355 nm) of a Nd-YAG laser (Surelite SLII-10/Continumm, 10 Hz, 5 ns) to generate excitation at a wavelength of 980 nm. The signal was dispersed by the same single monochromator (0.3 m) and the Tb^{3+}:$^5D_4 \rightarrow {}^7F_5$ UC luminescence decay curves were recorded using the PMT and a digital oscilloscope (TekTronix/TDS380) to estimate the Tb^{3+}:$^5D_4 \rightarrow {}^7F_5$ UC luminescence rise and decay times. All spectroscopic measurements were obtained at room temperature.

RESULTS AND DISCUSSION

Absorption spectra and Judd-Ofelt analysis

Figure 1 presents the absorption spectrum of 1.0Yb+2.0Tb co-doped CaLiBO glass in the 250-1500 nm range. This spectrum is also representative for all the samples. The spectrum presents the typical Tb^{3+} bands in regards to line shapes and wavelengths. The electronic levels of Tb^{3+}, excited by transitions from $^7F_6$ ground state are indicated, as well as the $^2F_{7/2} \rightarrow {}^2F_{5/2}$ transition of Yb^{3+} at 980 nm. The absorption coefficient in the NIR referring to the $^2F_{7/2} \rightarrow {}^2F_{5/2}$ transition of Yb^{3+} (980 nm) as a function of the nominal Yb^{3+} concentration had a linear dependence, and it is an indication of the successful incorporation of Yb^{3+} ions, for the prepared glass samples (not shown here).

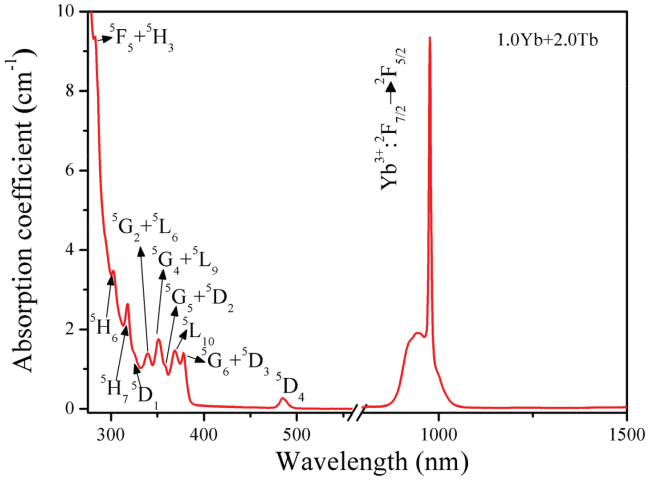

Figure 1. *Room temperature representative ground state absorption spectrum of 1.0Yb+2.0Tb co-doped glass sample. The transitions from ground states $^7F_6$ and $^2F_{7/2}$ are indicated*

In order to analyze the radiative properties of the Tb^{3+} ions, such as the total radiative transition rate between ions, luminescence branching ratios and radiative lifetimes, the well-established Judd-Ofelt (JO)[24,25] theory was applied. The Ω_λ intensity parameters ($\lambda = 2$, 4, 6) are extracted by the experimental and calculated oscillator strengths for each ground state absorption transition.

The experimental oscillator strength is obtained from the absorption spectrum according to the following equation (1):

$$F_{exp} = \frac{mc}{\pi e^2 N} \int \alpha(\nu)\, d\nu \quad (1)$$

The oscillator strength calculated contains the reduce matrix element of the given transition, and the Ω_λ parameters, and is given by the equation (2):

$$F_{cal} = \frac{8\pi^2 m}{3h} \frac{\nu}{2J+1} \left[\frac{(n^2+2)^2}{9n} \sum_{\lambda=2,4,6} \Omega_\lambda \left| \langle aJ \| U^\lambda \| bJ' \rangle \right|^2 + n^3 \left(\frac{\hbar}{2mc} \right)^2 \left| \langle aJ \| L + 2S \| bJ' \rangle \right|^2 \right] \quad (2)$$

In these equations, m is the electron mass, c is the speed of light, e is the electron charge, N is the number of doping ions per cm^3, $\int\alpha(\nu)$ is the area of the absorption band, n is the refractive index, h is the Planck constant, $\hbar$ is the reduced Planck constant, ν is the transition frequency, and J is the ground state quantum number. The first term in parentheses of equation (2) accounts for the electric dipole contributions, where $\langle aJ \| U^\lambda \| bJ' \rangle$ are the reduced matrix elements of the tensor operator U^λ of rank λ, corresponding to transitions from $\langle aJ|$ to $|bJ'\rangle$ to states. The matrix elements do not depend on the chemical environment and can be found in the literature.[26] The second term corresponds to the magnetic dipole contributions, with $L + 2S$ being the magnetic dipole operator.

Once the intensity parameters are determined, they can be used to calculate the total radiative transition rate between two levels, a and b, which can be obtained through the following expression:

$$A(aJ;bJ') = \frac{64\pi^4 E^3}{3(2J+1)h} \left[\frac{(n^2+2)^2}{9n} e^2 \sum_{\lambda=2,4,6} \Omega_\lambda \left| \langle aJ \| U^\lambda \| bJ' \rangle \right|^2 + n^3 \left(\frac{e\hbar}{2mc} \right)^2 \left| \langle aJ \| L + 2S \| bJ' \rangle \right|^2 \right] \quad (3)$$

In which is the average transition energy in cm^{-1} and J is the total angular momentum of the emitting level. The luminescence branching ratios and the radiative lifetime are given by:

$$\beta(aJ;\, bJ') = \frac{A(aJ;\, bJ')}{\sum_{J'} A(aJ;\, bJ')} \quad (4)$$

and

$$\tau_{rad} = \frac{1}{\sum_{S,L,J} A(aJ;\, bJ')}, \quad (5)$$

respectively.

The absorption spectrum obtained for a sample with 2.0Tb was used to obtain the Ω_λ intensities parameters, where $\lambda = 2, 4, 6$ for the CaLiBO glass doped with Tb^{3+} ions.

Table 1 presents the experimental and calculated oscillator strengths for the $J \rightarrow J'$ absorption transitions from the ground $^7F_6$ state to the excited levels, obtained using equations 1 and 2. The root-mean square (RMS) error for oscillator strengths was 1.8%. We determined the intensity parameters Ω_λ for CaLiBO:Tb^{3+}: $\Omega_2 = 15.5 \times 10^{-20}$ cm^2, $\Omega_4 = 1.90 \times 10^{-20}$ cm^2 and $\Omega_6 = 3.69 \times 10^{-20}$ cm^2.

The radiative transition rates considering the electric and magnetic dipole contributions, branching ratios and radiative lifetimes of the $^5D_4$ and $^5D_3$ levels are given in Tables 2 and 3, respectively.

Luminescence

The visible Stokes luminescence spectra were obtained after direct excitation into the $^5D_1$ energy level of Tb^{3+} ions at 325 nm. Figure 2 shows the corresponding spectrum for the 1.0Yb+0.5Tb co-doped glass. Regarding the line shape and wavelength positions, this spectrum is representative for the glasses with different Yb^{3+} doping

Table 1. Absorption transition of Tb^{3+} ion, wavelength (λ), and experimental and calculated oscillator strength (F_{exp} and F_{cal})

Transition (J →J´)	λ (nm)	F_{exp} (10^{-6})	F_{cal} (10^{-6})
$^7F_6 \rightarrow {}^7F_3$	2204	0.99	0.99
$^7F_6 \rightarrow {}^7F_{0,1,2}$	1921	2.22	2.20
$^7F_6 \rightarrow {}^5D_4$	485	0.06	0.05
$^7F_6 \rightarrow {}^5G_6+{}^5D_3$	378	0.28	0.25
$^7F_6 \rightarrow {}^5L_{10}$	369	0.62	0.66
$^7F_6 \rightarrow {}^5G_5+{}^5D_2$	359	0.24	0.24
$^7F_6 \rightarrow {}^5G_4+{}^5L_9$	351	0.66	0.66
$^7F_6 \rightarrow {}^5G_2+{}^5L_6$	339	0.12	0.11
$^7F_6 \rightarrow {}^5H_7$	318	0.48	0.50
$^7F_6 \rightarrow {}^5H_6$	304	0.34	0.33

Table 2. Transitions of Tb^{3+}:$^5D_4$ emitter level, emission wavelength ($\lambda_{emission}$), radiative transitions probabilities by electric dipole (A_{de}), radiative transitions probabilities by magnetic dipole (A_{dm}), branching ratios (β) and radiative lifetime (τ_{rad})

Transition ($^5D_4$→...)	$\lambda_{emission}$ (nm)	A_{de} (s^{-1})	A_{dm} (s^{-1})	$\beta_{JJ'}$(%)
$^5D_4 \rightarrow {}^7F_0$	680	2.6	0.0	0.5
$^5D_4 \rightarrow {}^7F_1$	671	4.0	0.0	0.8
$^5D_4 \rightarrow {}^7F_2$	649	17.5	0.0	3.3
$^5D_4 \rightarrow {}^7F_3$	622	40.7	4.6	8.5
$^5D_4 \rightarrow {}^7F_4$	586	16.5	0.6	3.2
$^5D_4 \rightarrow {}^7F_5$	544	360.0	39.2	74.7
$^5D_4 \rightarrow {}^7F_6$	488	47.9	0.0	9.0

Total radiative transition probability A_T = 534 s^{-1}; Radiative lifetime of the $^5D_4$ level τ_{rad} = 1.87 ms

Table 3. Transitions of Tb^{3+}:$^5D_3$ emitter level, emission wavelength ($\lambda_{emission}$), radiative transitions probabilities by electric dipole (A_{de}), radiative transitions probabilities by magnetic dipole (A_{dm}), branching ratios (β) and radiative lifetime (τ_{rad})

Transition ($^5D_3$→...)	$\lambda_{emission}$ (nm)	A_{de} (s^{-1})	A_{dm} (s^{-1})	$\beta_{JJ'}$(%)
$^5D_3 \rightarrow {}^5D_4$	1737	53.8	0.0	6.4
$^5D_3 \rightarrow {}^7F_1$	482	58.7	0.0	6.9
$^5D_3 \rightarrow {}^7F_2$	471	83.4	11.9	11.3
$^5D_3 \rightarrow {}^7F_3$	460	45.7	1.7	5.6
$^5D_3 \rightarrow {}^7F_4$	438	387.7	51.6	52.2
$^5D_3 \rightarrow {}^7F_5$	418	87.2	0.0	10.4
$^5D_3 \rightarrow {}^7F_6$	381	60.5	0.0	7.2

Total radiative transition probability A_T = 842 s^{-1}; Radiative lifetime of the $^5D_3$ level τ_{rad} = 1.18 ms

concentrations. As observed, a dominant green emission band with a peak centered at approximately 544 nm was identified and assigned to the Tb^{3+}:$^5D_4 \rightarrow {}^7F_5$ emitter level. The Tb^{3+}:$^5D_4 \rightarrow {}^7F_{6,4,3}$ emitter levels were also identified with peak emission bands centered at 488, 586 and 622 nm, respectively.

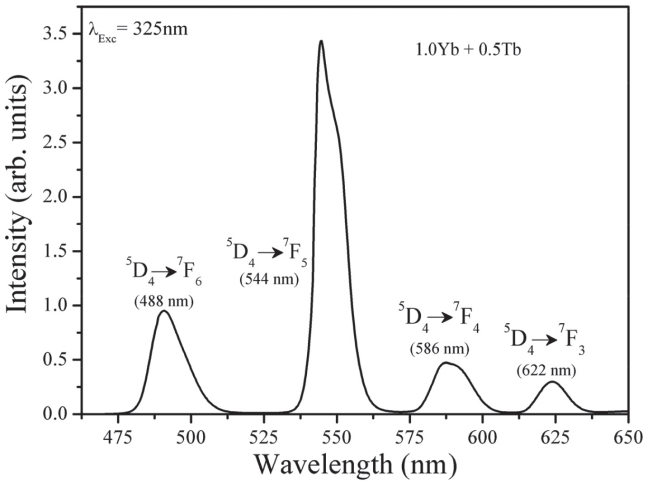

Figure 2. *Visible Stokes luminescence spectrum of the 1.0Yb+0.5Tb co-doped CaLiBO glass under λ_{Exc}=325 nm excitation*

The visible Stokes luminescence is reduced by a factor of 2 with an increase in the concentration of Yb^{3+} ions from (0.1 to 2.5) %mol, and NIR luminescence in the 950-1100 nm range from Yb^{3+} ions is enhanced nearly 17 times (not shown here). This result is explained by the DC process from Tb^{3+} to Yb^{3+}, as discussed in our previous article.[20] In that work, for the 0.0Yb+0.5Tb single-doped glass, after excitation at 488 nm and monitoring the Tb^{3+}:$^5D_4$ level at 544 nm, decay time was significantly higher, 2.38 ms than the Tb^{3+}: $^5D_4$ level radiative lifetime, 1.87 ms obtained in this work using Judd-Ofelt calculations (see Table 2). This difference in times could be explained in terms of an energy migration between Tb^{3+} ions, which induces a lengthening on the $^5D_4$ emitter level.

Upconversion emission studies

An analysis of the UC luminescence for the Yb^{3+}-Tb^{3+} co-doped CaLiBO glasses with excitation at 980 nm was performed. Figure 3 shows a simplified energy level diagram of the Yb^{3+} and Tb^{3+} ions with the relevant optical transitions. The UC through cooperative energy transfer (CET), the Yb^{3+}-Tb^{3+} cross-relaxation (CR) and (ESA) excited state absorption processes are indicated by dotted lines. The

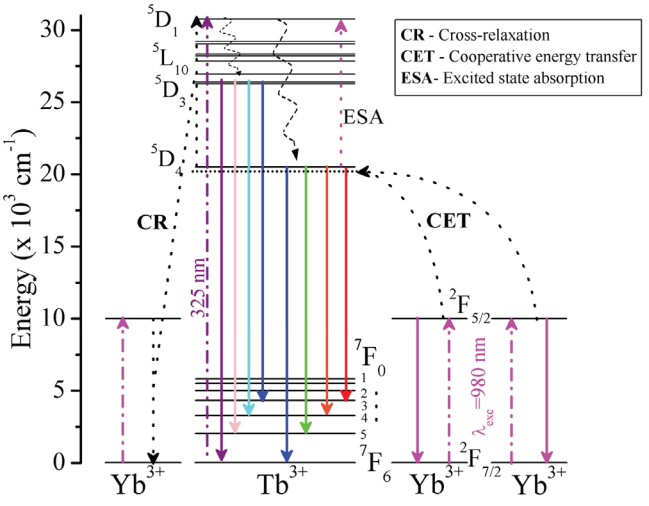

Figure 3. *Energy level diagrams of Yb^{3+} and Tb^{3+} ions. The UC through cooperative energy transfer (CET), Yb^{3+}-Tb^{3+} cross-relaxation (CR), and excited state absorption (ESA) processes are indicated by dotted lines. The non-radiative relaxation processes, excitation and emission transitions are indicated by dashed, dashed-dotted and solid lines, respectively*

non-radiative relaxation processes, excitation and emission transitions are indicated by dashed, dashed-dotted and solid lines, respectively.

The UC luminescence spectrum of the 1.0Yb+0.5Tb co-doped sample is presented in Figure 4 (a). The position and shape of the emission bands are consistent with those obtained upon direct excitation at 325 nm of the Tb^{3+}:$^5D_1$ level (Figure 3). A quadratic dependence on the excitation power at λ_{exc}=980 nm was observed in a log-log plot (not shown here) for the UC emission bands associated with the Tb^{3+}:$^5D_4 \rightarrow ^7F_J$, J = 3, 4, 5, and 6 emitter levels. This indicates that the absorption of two NIR photons results in the emission of one visible photon, as shown in Figure 3. Is important to mention that the CET process is not resonant. This process is mediated by phonons (thermal energy) to bridge the electronic energy gap between the Tb^{3+}: $^5D_4$ level and two times the lowest crystal field level of Yb^{3+}: $^2F_{5/2}$.[10,11]

The dependence of the peak intensity with Yb^{3+} concentration of the emission band centered at 544 nm (Tb^{3+}:$^5D_4 \rightarrow ^7F_5$ emitter level) via the UC process is shown in the inset of Figure 4 (a). In this inset, the Tb^{3+}:$^5D_4 \rightarrow ^7F_5$ UC luminescence increases nearly 68 times, with Yb^{3+} doping up to 2.5 %mol due to the increase in the number of Yb^{3+} activator ions; however, there is a quenching in the intensity for higher Yb^{3+} concentrations (> 2.5 %mol, indicating losses due to the Yb^{3+}-Tb^{3+} CR processes (see Figure 3). This is even if the energy transfer probability from Yb^{3+} to Tb^{3+}, extracted from time-resolved measurements, increases with Yb^{3+} concentration (as will be shown below). Figure 4 (b) shows the UC luminescence spectra of the xYb+0.5Tb co-doped samples in the UV-blue region (monitoring the $^5D_3$ level). The Tb^{3+}:$^5D_3 \rightarrow ^7F_{3,4,5,6}$ transitions are indicated, and an increase of the UC intensity can be observed. Moreover, the CR and ESA processes (see Figure 3) are confirmed by the curves of UC intensity versus pump power, monitoring the Tb^{3+}:$^5D_3 \rightarrow ^7F_4$ transition (not shown here). The emission around 440 nm presents a slope coefficient of 3, confirming the three-photon absorption mechanism that excites the Tb^{3+}:$^5D_3$ level.

UC luminescence kinetic response of Tb^{3+}

Time-resolved measurements enable the extraction of further information regarding the energy transfer process involved. We attempted to estimate the energy transfer probability from Yb^{3+} to Tb^{3+}, and the efficiency of the processes that depopulate the Tb^{3+}:$^5D_4$ level after resonantly pumping the Yb^{3+}:$^7F_{5/2}$ level. The analysis of the temporal evolution of the luminescence, specifically the rising feature after a short pulse, is a well-known fingerprint of an energy transfer process that does not require light to proceed, and therefore continues after the laser pulse.[10] Thus, the Tb^{3+}:$^5D_4 \rightarrow ^7F_5$ (544 nm) UC luminescence kinetics was studied as a function of the Yb^{3+} doping concentration. These measurements enable a description of the Tb^{3+} UC processes.

Figure 5 shows the normalized Tb^{3+}:$^5D_4 \rightarrow ^7F_5$ (544 nm) UC luminescence kinetics after pumping the Yb^{3+}:$^7F_{5/2}$ level at 980 nm using a 5-ns pulsed laser as excitation source. The inset in Figure 5 shows the first millisecond following the laser pulse. It should be noted that the rise part of the Tb^{3+}:$^5D_4 \rightarrow ^7F_5$ (544 nm) UC luminescence transient rose slowly from zero intensity after the laser pulse. The rise part of the transient was strongly affected by the Yb^{3+} concentration. In addition, the decay part of the transient exhibited non-exponential behavior.

The results indicate that the origin of the Tb^{3+}:$^5D_4 \rightarrow ^7F_5$ (544 nm) UC luminescence is due to a CET process from two Yb^{3+} ions to one Tb^{3+} ion. Thus, in accordance with Salley *et al.*,[27] the transients can be fitted using the following equation (6):

$$I(t) = A\left(e^{-\frac{t}{\tau_1}} - e^{-\frac{t}{\tau_2}}\right) \quad (6)$$

where τ_1 and τ_2 represent the decay and rise times of the transient, respectively. τ_1 provides information about the radiative and non-radiative process in the acceptor ion and the inverse of τ_2 ($W_{ET} = 1/\tau_2$) provides the energy transfer probability from the donor to the acceptor ion. Note that we have successfully employed equation (6) to estimate the energy transfer probability between Tb^{3+} and Yb^{3+} ions in our previous work.[11]

Therefore, τ_1 decreases from 1.64 to 0.79 ms and W_{ET} increases from 6.7×10^3 s^{-1} to 45.5×10^3 s^{-1} with Yb^{3+} doping in the range of 0.1-7.0 %mol (see Table 4). In the work reported by Terra *et al.*,[11] the mechanisms involved in the UC process in Yb^{3+}+Tb^{3+} co-codoped aluminosilicate glasses were analyzed. In that work, the values reported for the UC luminescence rise times are in the range from 20 to 65 microseconds for the temperature range from 123 to 473 K. The inverse of those rise times results in values of probability of energy transfer in the range from 50×10^3 to 15.4×10^3 s^{-1}, which are comparable to the values calculated in the present work. On

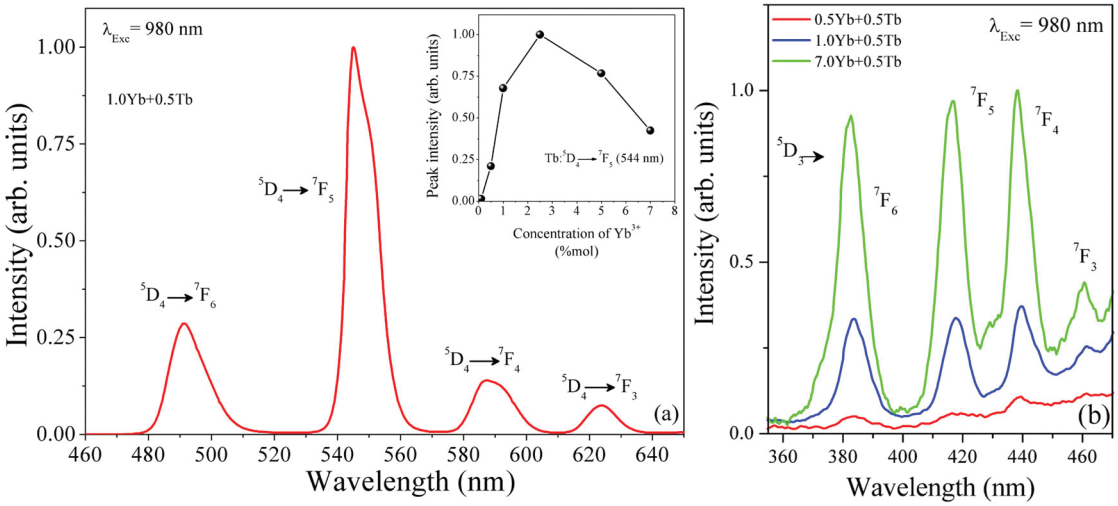

Figure 4. *(a) Tb^{3+} UC luminescence spectrum in the visible region of the 1.0Yb+0.5Tb co-doped CaLiBO glass upon excitation at λ_{Exc}=980 nm. The inset presents the dependence of the peak intensity with Yb^{3+} doping concentration of the emission band centered at 544 nm (Tb^{3+}:$^5D_4$ $^7F_5$ emitter level) via the UC process. (b) UV-blue UC luminescence spectra for the samples xYb+0.5Tb with (x=0.5, 1.0, 7.0). The Tb^{3+}:$^5D_3$ ^7F_J, J = 6, 5, 4, and 3 emitter levels are indicated, excitation at λ_{Exc}=980 nm*

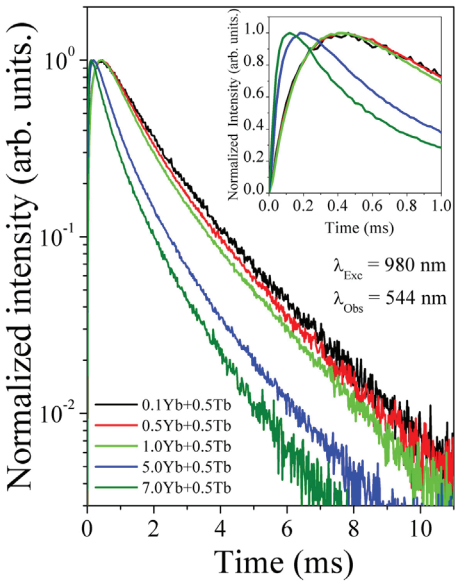

Figure 5. *Kinetic response of Tb^{3+} UC luminescence for the samples xYb+0.5Tb with (x = 0.1, 0.5, 1.0, 5.0, 7.0) upon excitation at λ_{Exc} = 980 nm, monitored at λ_{Obs} = 544 nm (Tb^{3+}:$^5D_4 \rightarrow ^7F_5$ emitter level). The inset shows the responses at the first millisecond after the laser pulse*

the other hand, in the work reported by Salley *et al.*,[27] studying the UC process in a Yb^{3+}+ Tb^{3+} co-codoped $SrCl_2$ crystal, they obtained an energy transfer probability value of the order of 6.9 × 10^3 s^{-1}, measured at 100 K. It can be seen that the W_{ET} values of this work and those of Terra are greater than that reported by Salley and this is understandable, since it is known that rare earth ions agglomerates are usually formed in glasses and not in crystals, which facilitates the energy transfer from one ion to another.

The non-exponential behavior of the decay part of the transient and the decrease of τ_1 with increasing Yb^{3+} concentration in this set of samples is due to the presence of non-radiative processes involved in the Tb^{3+}:$^5D_4$ level. The most likely non-radiative process that depopulates the Tb^{3+}:$^5D_4$ level after pumping the Yb^{3+}:$^7F_{5/2}$ level is the Yb^{3+}-Tb^{3+} CR (as depicted in Figure 3).

Table 4. Tb^{3+}:$^5D_4 \rightarrow ^7F_5$ (544 nm) UC luminescence decay time (τ_1), rise time (τ_2), energy transfer probability ($W_{ET} = 1/\tau_2$) and the efficiency of processes that depopulate the Tb^{3+}:$^5D_4$ level (η) in Yb^{3+}-Tb^{3+} co-doped CaLiBO glasses upon excitation at 980 nm as a function of the concentration of Yb^{3+}. The luminescence decay time upon excitation at 488 nm is also shown for comparison[20]

*x*Yb+0.5Tb (% mol)	τ_1 (ms)	Decay time (ms) with λ_{Exc} = 488 nm*	τ_2 (μs)	W_{ET} (x10^3 s^{-1})	η (%)
0.1	1.64	2.37	149	6.7	31
0.5	1.52	2.33	149	6.7	36
1.0	1.38	2.27	149	6.7	42
2.5	1.19	2.03	112	8.9	50
5.0	0.97	1.62	47	21.3	59
7.0	0.79	1.32	22	45.5	67

For comparison purposes, the Tb^{3+}:$^5D_4 \rightarrow ^7F_5$ (544 nm) decay times after excitation at 488 nm (extracted from our previous DC experiment)[20] are shown in Table 4. Note that these decay times are considerably higher than those estimated in the UC experiment analyzed here. These results indicate that the CR process is present after excitation at 980 nm.

The efficiency of the CR process (Figure 3) that depopulates the Tb^{3+}:$^5D_4$ level after pumping the Yb^{3+}:$^7F_{5/2}$ level could be calculated using the following equation (7):

$$\eta = 1 - \frac{\tau_{xYb+Tb}}{\tau_{Tb}} \quad (7)$$

where τ_{xYb+Tb} is the Tb^{3+}:$^5D_4 \rightarrow ^7F_5$ (544 nm) UC luminescence decay time in the presence of Yb^{3+}, and τ_{Tb} = 2.38 ms is the Tb^{3+}:$^5D_4 \rightarrow ^7F_5$ (544 nm) luminescence decay time for the Tb^{3+} singly doped sample (0.5 %mol) after excitation at 488 nm (see Ref[20]). These values are summarized in Table 4, where η is observed to increase from 31% to 67% when the concentration of Yb^{3+} ions increases, indicating that the CR process is efficient.

We have observed that the Tb^{3+} UC luminescence slowly rises over time in our samples. The origin of the Tb^{3+} UC luminescence is due to a CET process in which two Yb^{3+} ions simultaneously transfer the energy to one Tb^{3+} ion ($2Yb^{3+}$:$^2F_{5/2}$; Tb^{3+}:$^7F_6 \rightarrow 2Yb^{3+}$:$^2F_{7/2}$; Tb^{3+}:$^5D_4$), as depicted in Figure 3.

CONCLUSIONS

This paper presents a qualitative and quantitative perspective on the study of the spectroscopic properties of Yb^{3+}-Tb^{3+} co-doped CaLiBO glasses, using absorption, luminescence and time-resolved measurements. Intensity parameters Ω_λ for CaLiBO:Tb^{3+} glass have been determined by the Judd–Ofelt method to be $\Omega_2 = 15{,}5 \times 10^{-20}$ cm^2, $\Omega_4 = 1{,}90 \times 10^{-20}$ cm^2 and $\Omega_6 = 3{,}69 \times 10^{-20}$ cm^2. These values were used to calculate spectroscopic properties, such as oscillator strengths, probabilities, and radiative lifetimes. The analyses covered herein showed that CaLiBO glass is a good host for high concentrations of Yb^{3+} and Tb^{3+} ions. The rise and decay times of the Tb^{3+}:$^5D_4 \rightarrow ^7F_5$ UC transient luminescence allowed for determination of the energy transfer probability and the efficiency of the processes that depopulate the Tb^{3+}:$^5D_4$ level after resonantly pumping the Yb^{3+}:$^7F_{5/2}$ level. The time-resolved measurements identified the origin of the Tb^{3+}:$^5D_4 \rightarrow ^7F_5$ UC luminescence as a cooperative energy transfer mechanism from two Yb^{3+} ions to one Tb^{3+} ion. The results suggest that Yb^{3+}-Tb^{3+} co-doped CaLiBO glasses are potential materials for applications in the form of optical converters.

ACKNOWLEDGMENTS

The authors acknowledge financial support from the following Brazilian Agencies: Coordenação de Aperfeiçoamento de Pessoal de Nível Superior (CAPES), Fundação de Amparo à Pesquisa do Estado de São Paulo (FAPESP) and Conselho Nacional de Desenvolvimento Científico e Tecnológico (CNPq).

REFERENCES

1. Escudero, A.; Becerro, A. I.; Carrillo-Carrión, C.; Núñez, N. O.; Zyuzin, M. V.; Laguna, M.; González-Mancebo, D.; Ocaña, M.; Parak, W. J.; *Nanophotonics* **2017**, *6*, 1568.
2. Yang, W.; Li, X.; Chi, D.; Zhang, H.; Liu, X.; *Nanotechnology* **2014**, *25*, 482001.
3. Borrero-González, L. J.; Terra, I. A. A.; Nunes, L. A. O.; Farias, A. M.; Barboza, M. J.; Rohling, J. H.; Medina, A. N.; Baesso, M. L.; *Appl. Phys. B: Lasers Opt.* **2012**, *107*, 415.
4. Dexter, D. L.; *Phys. Rev.* **1957**, *108*, 630.
5. Auzel, F.; *C. R. Seances Acad. Sci., Ser. B* **1966**, *263*, 819.
6. Livanova, L. D.; Saitkulo, I. G.; Stolov, A. L.; *Soviet Physics – Solid State* **1969**, *11*, 750.

7. Ostermayer, F. W.; Van Uitert, L. G.; *Phys. Rev. B* **1970**, *1*, 4208.
8. Martín, I. R.; Yanes, A. C.; Méndez-Ramos, J.; Torres, M. E.; Rodríguez, V. D.; *J. Appl. Phys.* **2001**, *89*, 2520.
9. Huang, L.; Yamashita, T.; Jose, R.; Arai, Y.; Suzuki, T.; Ohishi, Y.; *Appl. Phys. Lett.* **2007**, *90*, 131116.
10. Salley, G. M.; Valiente, R.; Güdel, H. U.; *J. Phys.: Condens. Matter.* **2002**, *14*, 5461.
11. Terra, I. A. A.; Borrero-González, L. J.; Nunes, L. A. O.; Belançon, M. P.; Rohling, J. H.; Baesso, M. L.; Malta, O. L.; *J. Appl. Phys.* **2011**, *110*, 083108.
12. Terra, I. A. A.; de Camargo, A. S. S.; Terrile, M. C.; Nunes, L. A. O.; *J. Lumin.* **2008**, *128*, 891.
13. Tripathi, G.; Rai, V. K.; Rai, S. B.; *Appl. Phys. B: Lasers Opt.* **2006**, *84*, 459.
14. Tripathi, H. B.; Kandpal, H. C.; Agarwal, A. K.; *Phys. Status Solidi A* **1979**, *52*, 697.
15. Joshi, J. C.; Joshi, B. C.; Pandey, N. C.; Belwal, R.; Joshi, J.; *J. Solid State Chem.* **1977**, *22*, 439.
16. Joshi, J. C.; Pandey, N. C.; Joshi, B. C.; BelWal, R.; Joshi, J.; *J. Non-Cryst. Solids* **1978**, *27*, 173.
17. Joshi, J. C.; Joshi, B. C.; Pandey, N. C.; Pandey, B. C.; Joshi, J.; *J. Solid State Chem.* **1978**, *26*, 179.
18. Tripathi, H. B.; Agarwal, A. K.; Kandpal, H. C.; Belwal, R.; *Solid State Commun.* **1978**, *28*, 807.
19. Tripathi, H. B.; Kandpal, H. C.; Agarwal, A. K.; Belwal, R.; *Chem. Phys. Lett.* **1978**, *57*, 50.
20. Terra, I. A. A.; Borrero-González, L. J.; Figueredo, T. R.; Almeida, J. M. P.; Hernandes, A. C.; Nunes, L. A. O.; Malta, O. L.; *J. Lumin.* **2012**, *132*, 1678.
21. Yamashita, T.; Ohishi, Y.; *J. Non-Cryst. Solids* **2008**, *354*, 1883.
22. Hoshina, T.; *Jpn. J. Appl. Phys. (1962-1981)* **1967**, *6*, 1203.
23. Colak, S.; Zwicker, W. K.; *J. Appl. Phys.* **1983**, *54*, 2156.
24. Ofelt, G. S.; *J. Chem. Phys.* **1962**, *37*, 511.
25. Judd, B. R.; *Phys. Rev.* **1962**, *127*, 750.
26. Carnall, W. T.; Fields, P. R.; Rajnak, K.; *J. Chem. Phys.* **1968**, *49*, 4447.
27. Salley, G. M.; Valiente, R.; Guedel, H. U.; *J. Lumin.* **2001**, *94*, 305.